Controls on advance of tidewater glaciers: Results from numerical modeling applied to Columbia Glacier

F. M. Nick,[1,2] C. J. van der Veen,[3,4] and J. Oerlemans[1]

Received 3 May 2006; revised 25 September 2006; accepted 29 January 2007; published 11 July 2007.

[1] A one-dimensional numerical ice flow model is used to study the advance of a tidewater glacier into deep water. Starting with ice-free conditions, the model simulates glacier growth at higher elevations followed by advance on land to the head of the fjord. Once the terminus reaches a bed below sea level, calving is initiated. A series of simulations was carried out with various boundary conditions and parameterizations of the annual mass balance. The results suggest that irrespective of the calving criterion and accumulation rate in the catchment area, it is impossible for the glacier terminus to advance into deeper water (>300 m water depth) unless sedimentation at the glacier front is included. The advance of Columbia Glacier, Alaska, is reproduced by the model by including ''conveyor belt'' recycling of subglacial sediment and the formation of a sediment bank at the glacier terminus. Results indicate slow advance through the deep fjord and faster advance in shallow waters approaching the terminal moraine shoal and the mouth of the fjord.

Citation: Nick, F. M., C. J. van der Veen, and J. Oerlemans (2007), Controls on advance of tidewater glaciers: Results from numerical modeling applied to Columbia Glacier, *J. Geophys. Res.*, *112*, F03S24, doi:10.1029/2006JF000551.

1. Introduction

[2] Tidewater glaciers are observed to go through cycles of slow advance followed by rapid retreat [e.g., *Post*, 1975; *Meier and Post*, 1987]. The recent dramatic retreat of many tidewater glaciers around the world has drawn major attention to the issue of the stability of calving glaciers. Examples of recent significant changes include the rapid thinning of many of the outlet glaciers in Greenland during the 1990s [*Abdalati et al.*, 2001], the dramatic retreat of Jakobshaven Isbræ to the head of its fjord in early 2002 [*Joughin et al.*, 2004], and the significant retreat of Columbia Glacier in Alaska since the early 1980s [*Meier and Post*, 1987; *Pfeffer et al.*, 2000].

[3] While some attempts have been made to develop models for calving [e.g., *Reeh*, 1968; *Hughes*, 1992; *van der Veen*, 1996; *Hughes and Fastook*, 1997; *Hanson and Hooke*, 2000, 2004], there is, at present, no theoretical model available that can explain the observations. It has been noted on many glaciers that the calving rate (volume of ice that breaks off from the glacier terminus per unit time and unit vertical area) increases with water depth at the terminus. *Brown et al.* [1982] and *Pelto and Warren* [1991] therefore proposed the water depth model in which the annual calving rate is linearly related to the water depth at the glacier terminus. On the other hand, *Meier and Post* [1987] and *van der Veen* [1996] argued that the water depth model is relevant only for glaciers that are almost in steady state. On the basis of observations made during the rapid retreat of Columbia Glacier, Alaska, as well as on several other grounded glaciers, *van der Veen* [1996] suggested that the position of the calving front is controlled by both water depth and ice thickness at the glacier terminus and presented the flotation model. In the flotation model the terminus position is defined as the point where the ice thickness exceeds the flotation thickness by an amount H_0. If the glacier thins, the terminus will retreat to a point where this condition is again satisfied. *Vieli et al.* [2001] modified the flotation criterion and defined the thickness in excess of flotation H_0 as a fraction of the flotation thickness. A recent modeling study by *Nick and Oerlemans* [2006] compared both the water depth and the flotation calving models, using a numerical model to simulate retreat and advance of tidewater glaciers with simplified geometries. They showed that although the flotation model is capable of simulating retreat and advance of some tidewater glaciers better than the water depth model, it fails to simulate a full cycle of glacier length variations when the glacier terminates into very deep water. Hence it is still unresolved whether a universally applicable calving model exists.

[4] Understanding the interaction between calving glaciers and climate is essential to interpret the past, to monitor the present, and to predict the future. *Clarke* [1987] suggested that calving glaciers are inherently unstable, with periodic cycles of advance and retreat that may be nearly independent of climate. Further, it has been shown that the advance/retreat behavior of tidewater glaciers is mainly a

[1]Institute for Marine and Atmospheric Research, Utrecht University, Utrecht, Netherlands.
[2]Currently at Department of Geography, University of Durham, Durham, UK.
[3]Byrd Polar Research Center and Department of Geological Sciences, Ohio State University, Columbus, Ohio, USA.
[4]Now at Department of Geography, University of Kansas, Lawrence, Kansas, USA.

0148-0227/07/2006JF000551

function of fjord geometry [*Mercer*, 1961], water depth at the glacier terminus [*Brown et al.*, 1982], and sedimentation at the glacier front [*Powell*, 1991]. The different terminus behavior of neighboring glaciers, which are derived from the same snowfield, suggests that their terminus advance or retreat is largely the result of internal dynamics rather than climatic changes. However, *Viens* [1995] showed that climate acts as a first-order control on the advance/retreat cycle by placing limitations on glacier advance and determining where the terminus reaches an equilibrium state during retreat (on the basis of observations of Alaskan tidewater glaciers). The above reveals that the diverse behavior of tidewater glaciers is likely the result of the complex interaction between internal dynamics and climate forcing. Therefore a better understanding of the processes controlling dynamics of tidewater glaciers is needed to make any interpretation of the past or prediction of future behavior of these glaciers.

[5] Tidewater glaciers may experience a continuous advance caused by a low-lying equilibrium line altitude (ELA) [*Mercer*, 1961] or because of the presence of a frontal sediment shoal which reduces water depth at the terminus and lowers calving rates [*Powell*, 1991]. The role of sediment deposition at the glacier terminus, allowing the glacier to advance, has been recognized in many previous studies [e.g., *Post*, 1975; *Alley*, 1991; *Powell*, 1991; *Hunter et al.*, 1996a; *Fischer and Powell*, 1998]. The extensive areas uncovered by glacier retreat during the last hundred years demonstrate that many glaciers are underlain by soft and poorly lithified sediments. Tidewater glaciers often advance over their own sediments, which are easily eroded and transported forward. *Powell* [1990] proposed that if the location of the glacier front is more or less stationary, morainal banks can form relatively fast: Sedimentation rates at such locations can easily be of the order of meters to tens of meters per year. Subsequently, *Alley* [1991] introduced a model describing a moraine shoal that moves with the advancing glacier front. *Oerlemans and Nick* [2006] presented a basic glacier sediment model in which the morainal shoal is forced to move with the advancing glacier front. Their model demonstrated that the feedback between sediment shoal and calving rates leads to a strongly nonlinear response to climate forcing.

[6] The objective of the present study is to identify processes most important in controlling the advance of tidewater glaciers, focusing on the extensively documented Columbia Glacier. A numerical flow line model is used to investigate whether glacier advance into its deep fjord is primarily driven and sustained by changes in climate forcing or whether other mechanisms such as the internal dynamics are the main controls on advance. To investigate the importance of sediment bank formation on the stability of the glacier terminus, we combined the numerical flow line model with a simple sedimentation model. Additionally, two calving formulations, the flotation model and the water depth model, are incorporated, and their predictions are compared. Available data for the historical advance of Columbia Glacier are used to assess how well the model applies to this glacier.

2. Columbia Glacier

[7] Located in south central Alaska, Columbia Glacier is the last of the major Alaskan tidewater glaciers to retreat from an extended position at the seaward end of its fjord. The glacier is currently about 52 km long, extending from 3050 m elevation in the western Chugach Mountains down to sea level, discharging icebergs into Columbia Bay in Prince William Sound. The glacier is grounded with a substantial amount of ice in the lower reach below sea level.

[8] A 1000 year advance of Columbia Glacier is documented by tree ring calendar dates from subfossil and living trees. During this advance the glacier expanded into forest along its fjord margins, burying trees in glacial sediments. These forests have been uncovered during the last two decades of retreat, and their tree ring data provide records of earlier advance into Columbia Bay as well as records of past climate conditions. The chronology shows an average advance rate of 36 m yr^{-1} between A.D. 1060 and 1808 with a significant stand-still or minor retreat circa A.D. 1450 [*Kennedy*, 2003]. Between 1800 and the early 1980s the position of the terminus was relatively stable, but in 1981, retreat began and has continued at an increasing rate [*Krimmel*, 1997; *Pfeffer et al.*, 2000]. During the last 25 years the terminus has receded 14 km.

[9] During the Little Ice Age (A.D. 1200–1900) the majority of Alaskan glaciers reached their Holocene maximum extensions. ELAs were lowered 150–200 m below present values [*Calkin et al.*, 2001]. *Barclay et al.* [1999] developed a 1000 year tree ring width chronology for the western Prince William Sound by using living and subfossil trees from glacier forefields. They showed that multidecadal long warm periods occurred around A.D. 1300, 1440, and possibly 1820 with cool intervals centered on A.D. 1400, 1660, and 1870.

[10] The rapid retreat of Columbia Glacier has been monitored on a regular basis since 1976 by aerial photogrammetry conducted by the U.S. Geological Survey [*Krimmel*, 1997, 2001]. Derived surface elevations and surface speeds are published [*Fountain*, 1982; *Krimmel*, 1987, 1992, 2001] for the period of 1976 until 2001. The bed topography of the lower reach is known from bathymetry, radio echo sounding, and boreholes [*Krimmel*, 2001; *Meier*, 1994]; few data are available for the catchment area of the glacier.

[11] The climate of Prince William Sound is characterized by mild winters and cool summers, with annual precipitation ranging from 1700 to 2400 mm. At higher altitudes, above 2500 m above sea level, the temperature remains below freezing except for a few days in mid-July [*Tangborn*, 1997]. The high precipitation rates, together with the high mountainous area, provide favorable conditions for glaciers to form and expand. The Columbia Glacier mass balance was measured, with stakes located approximately at 100 m elevation intervals, in 1977–1978 by the U.S. Geological Survey [*Mayo et al.*, 1979]. By using observed low-altitude temperature and precipitation, *Tangborn* [1997] provided a 50 year (1949–1996) modeled mass balance as a function of altitude and time.

3. Methods and Materials

[12] This section summarizes the time-evolving model and the processes included in the model.

3.1. Model Description

[13] The flow line model calculates the change in ice thickness H and ice velocity U along a central flow line

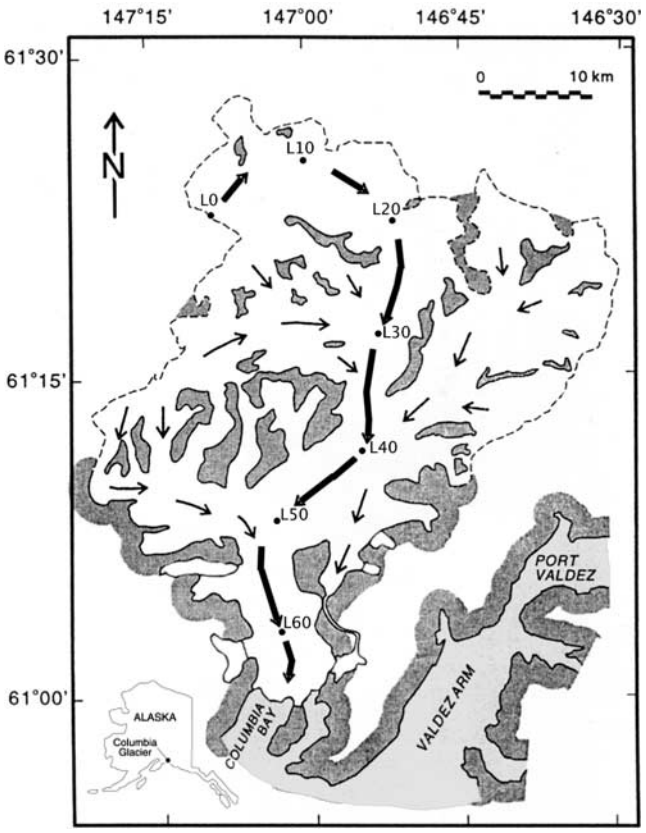

Figure 1. Map of Columbia Glacier. Dark shading represents exposed rock, and light shading indicates open water. The thick arrows show the central flow line, and the thin ones denote direction of the ice flow in side branches.

[*Oerlemans*, 2001; *van der Veen and Payne*, 2004]. Evolution of the glacier thickness is described by the vertically and laterally integrated continuity equation [*van der Veen*, 1999]

$$\frac{\partial H}{\partial t} = -\frac{1}{W}\frac{\partial (WHU)}{\partial x} + B, \tag{1}$$

where t is time, x is distance along the central flow line, B is the surface mass balance, and W is the glacier width. Equation (1) is solved on a discrete grid using the finite difference method. A moving grid is used, which allows the position of the terminus to be determined with high accuracy. At each time step a new grid is defined to fit the new glacier length. For further details, see *Nick and Oerlemans* [2006].

3.2. Glacier Geometry

[14] The model is essentially one-dimensional, but three-dimensional geometry is implicitly taken into account through the parameterization of the cross-sectional geometry along the flow line (thick arrows in Figure 1). This geometry is determined by two parameters, the bed elevation and glacier width. The bed elevation is provided by *Krimmel* [2001, Figure 11]. For the last 20 km of the fjord the bed elevation suggested by *O'Neel et al.*, [2006] is used (Figure 2a). An approximate glacier width along the central flow line was estimated from a topographic map of Columbia Glacier. The tributaries are taken into account in such a way that the surface elevation distribution is not distorted too much (Figure 2b). The glacier width may also vary with glacier thickness, becoming wider when the glacier thickens. There are insufficient data available on the cross-sectional profile of the fjord basin. Therefore two possible cross-sectional geometries, rectangular and trapezoidal [*Oerlemans*, 2001], are considered in the model.

3.3. Ice Velocities

[15] The ice velocity is expressed as a velocity averaged over the cross section and includes contributions from basal sliding U_s and internal ice deformation U_d. In this model the vertical shear stress is related to strain rate according to Glen's flow law [*Glen*, 1955], which yields [*Paterson*, 1981]

$$U_d = \frac{2A}{n+1} H S_d^n. \tag{2}$$

The typical value of the flow law exponent $n = 3$ [*Alley*, 1992] and a rate factor $A = 1 \times 10^{-7}$ kPa^{-3} yr^{-1}, corresponding to ice near the freezing point [*van der Veen*, 1999, Figure 2.6], are used. The driving stress S_d is defined as

$$S_d = -\rho_i g H \frac{\partial h}{\partial x}, \tag{3}$$

where $\partial h/\partial x$ is surface slope and $g = 9.8$ m s^{-2} is the gravitational acceleration.

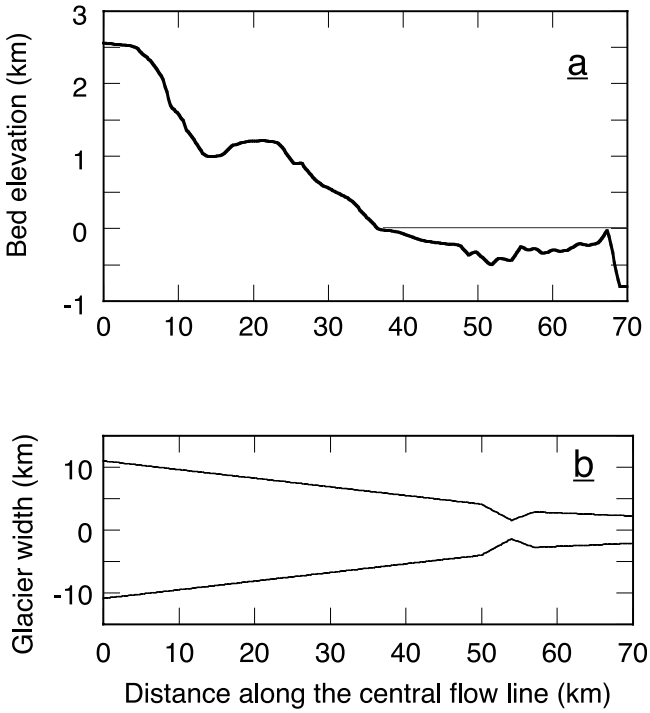

Figure 2. (a) Bed elevation and (b) glacier width along the central flow line.

[16] It has been shown that most of the flow resistance on the lower reach of Columbia Glacier is due to basal drag and the rest is mainly due to lateral drag; gradients in longitudinal stress contribute little to the resistance to flow [*van der Veen and Whillans*, 1993; *O'Neel et al.*, 2006]. Lateral drag could be included in the model by introducing a shape factor [*Nye*, 1965; *Bindschadler*, 1983]. However, considering the geometry of Columbia Glacier (with a large width-to-height ratio), these effects are probably too small to be crucial for the large-scale flow of glacier and are therefore ignored in the present model.

[17] The fast flow of Columbia Glacier is primarily due to high sliding velocities [*Meier*, 1994; *Kamb et al.*, 1994]. It has been recognized that subglacial water pressure plays an important role in sliding process [*Weertman*, 1964; *Budd et al.*, 1979; *Iken*, 1981; *Bindschadler*, 1983]. A modified Weertman-type sliding velocity [*Budd et al.*, 1979; *Bindschadler*, 1983] is adopted here

$$U_s = A_s \frac{S_b^m}{N_{\text{eff}}^p}. \tag{4}$$

The effective pressure N_{eff} is equal to the difference between ice overburden pressure P_i and subglacial water pressure P_w. A high subglacial water pressure or a thin glacier front reduces the effective basal pressure which leads to enhanced sliding. Basal drag S_b is set equal to driving stress S_d. *Bindschadler* [1983] compared four basal sliding formulations suggested by theoretical and experimental studies and concluded that equation (4) provides the best fit to field measurements. He estimated the empirical parameters $A_s = 84$ m yr^{-1} bar^{1-m}, $m \approx 3$, and $p = 1$ using the best fit between inferred and predicted velocities along Variegated Glacier. In this study we used the observed surface and bed elevation and ice surface velocity of the lower reach of Columbia Glacier ($\sim$15 km) obtained from data during the glacier retreat collected by the U.S. Geological Survey [*Brown et al.*, 1982; *Krimmel*, 1997, 2001; *Meier et al.*, 1985; *Sikonia*, 1982]. There are no direct measurements of sliding velocity available, but the observed surface velocity can be considered as an estimate of the sliding velocity because fast flow in the lower reach is predominantly associated with basal sliding. Using multivariate regression, a best fit between calculated and observed velocities was found for $A_s = 9.2 \times 10^6$ m yr^{-1} Pa$^{0.5}$, $m = 3$, and $p = 3.5$. The basal pressure cannot exceed the ice overburden pressure as this would correspond to a net upward force and

$$(P_w)_{\max} = \rho_i g H, \tag{5}$$

where ρ_i is the ice density. At the glacier front the terminus may be close to flotation [*Meier et al.*, 1994; *Meier*, 1994], which means that the effective pressure becomes very small, leading to the sliding velocity becoming too large and resulting in numerical instabilities. Therefore a minimum effective pressure of 150 kPa is prescribed. This limit is in the range measured at the lower reach of Columbia Glacier during its retreat [*van der Veen*, 1995]. Another model assumption is that there exists a full and easy water connection between the glacier base and the adjoining sea [*Lingle and Brown*, 1987], so that the subglacial water pressure can be estimated from

$$P_w = \rho_w g b, \tag{6}$$

where ρ_w is the water density and b denotes height of the ice column below sea level.

[18] Although the sliding formulation is obtained from data during the glacier retreat, it can be also used in the model to simulate the glacier advance. Equation (4) yields high velocities during glacier retreat as has been observed, but during advance, velocities predicted by equation (4) remain moderate because the glacier thickness is large and thus the effective pressure is large. It will be shown that modeled advance does not depend on basal sliding velocity.

3.4. Surface Mass Balance

[19] The surface mass balance is prescribed as a linear function of elevation

$$B = \beta(h - \text{ELA}), \tag{7}$$

where β is a constant balance gradient, ELA is the equilibrium line altitude, and h is surface elevation. On the basis of mass balance measurements on Columbia Glacier made in 1977–1978 by the U.S. Geological Survey [*Mayo et al.*, 1979] a high balance gradient $\beta \sim 0.01$ yr^{-1} was chosen for the model simulations. The modeled 1949–1996 mass balance of Columbia Glacier suggests an ELA of $\sim$1000 m [*Tangborn*, 1997]. During the Little Ice Age in Alaska, ELAs were depressed by 150–200 m below the present-day [*Calkin et al.*, 2001]; therefore the mean value of ELA = 900 m was applied to reproduce glacier advance.

3.5. Boundary Conditions

[20] The up-glacier model boundary is at the ice divide, so there is no ice flux into the model domain; therefore the ice velocity at the first grid point is set to zero, and the ice thickness at this grid point is extrapolated from the neighboring points. At the downstream end of the glacier the calculated ice velocity at the terminus tends to become unrealistically high because of the large slope from the glacier surface to sea level. For that reason the terminus ice velocity was set equal to the ice velocity at the first upstream grid point.

[21] To incorporate the two calving models, two different boundary conditions at the downstream end of the glacier are prescribed. For the flotation model the glacier thickness at the terminus cannot be less than a given limit H_c, which depends on the local water depth. *Vieli et al.* [2001] defined the critical thickness H_c as a small fraction q_0 of the flotation thickness plus the flotation thickness as

$$H_c = -\frac{\rho_w}{\rho_i}(1 + q_0)d, \tag{8}$$

where d is the bed elevation at the calving front (negative where the bed is below sea level). For Columbia Glacier, $q_0 = 0.15$ is suggested by *Vieli et al.* [2001]. The position of the terminus, at each time step, is shifted to the point where the ice thickness equals H_c. The actual position of

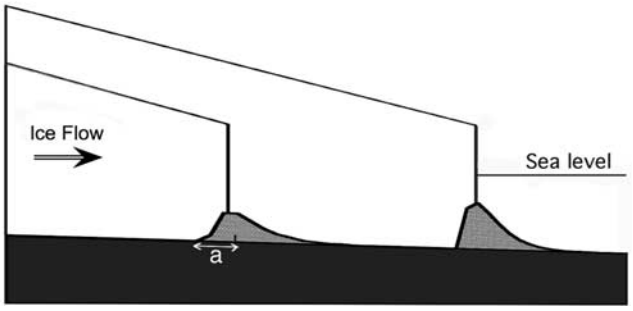

Figure 3. Forward movement of the growing moraine shoal in front of the glacier.

the terminus is determined by interpolating between values of two neighboring grid points with ice thicknesses larger and smaller than H_c. Thereafter new grid points are defined to fit the updated glacier length.

[22] In the water depth model the calving rate U_c is linearly related to the water depth at the terminus

$$U_c = -\alpha d. \tag{9}$$

To simulate advance of Columbia Glacier, the coefficient $\alpha = 10\ \mathrm{yr}^{-1}$ is used [*van der Veen* 1995, Figure 12]. The terminus position changes in response to the imbalance between ice velocity and calving rate [*Meier*, 1994, 1997]

$$\frac{dL}{dt} = U_f - U_c, \tag{10}$$

where L is the glacier length. At each time step the position of the terminus is obtained from the ice velocity at the terminus U_f minus the calving rate.

3.6. Sediment Model

[23] There are several processes which regulate the growth and collapse of the sedimentation pile at the glacier front, glacial debris deposition, glaciofluvial sediment deposition, bed deformation, calve dumping, etc. [*Hunter et al.*, 1996a]. Considering these processes, it is reasonable to assume that the deposition rate is largest at the glacier front and drops off smoothly with distance away from the glacier front [*Oerlemans and Nick*, 2006]. A moraine shoal is assumed at the glacier front, which moves forward with the advancing front. The sediment supply is continuous, and the volume of the shoal increases over time. The height of the shoal along the flow line is described as

$$s(x) = \begin{bmatrix} \dfrac{x-(L-a)}{a^2} & 0 & x < L-a \\ & e^{\frac{(x-(L-a))}{a}} Q(t) & x > L-a \end{bmatrix}, \tag{11}$$

where a = 300 m determines the shoal width, chosen to provide a reasonable geometry for the morainal shoal (Figure 3). Admittedly, this value is not supported by any observational evidence or theoretical study. $Q(t)$ is the total amount of sediment along the flow line supplied by the advancing glacier. This amount varies with glacier length and time:

$$Q(t) = \int_0^t q \quad L dt \tag{12}$$

in which q is the average erosion rate under the glacier; the value $q = 4\ \mathrm{mm\ yr}^{-1}$ is used, which is in the range of values obtained from morainal banks in Glacier Bay, Alaska [*Hunter et al.*, 1996b].

[24] As the glacier front terminates into water, at each time step, a new bed profile is determined by adding $s(x)$ to the original bed profile (Figure 2a). Taking into account that the last part of the fjord is a morainal shoal made during glacier advance, the modified bed elevation cannot become higher than the original bed profile near the mouth of the fjord, where the water depth is less than 60 m.

4. Model Experiments

[25] A series of simulations was conducted to assess whether the formation of a proglacial moraine bank is a necessary condition for advance of Columbia Glacier into its deep fjord.

4.1. Glacier Advance Without Moraine Bank

[26] The simulation starts from ice-free conditions; a large surface mass balance, ELA = 100 m in equation (7), forces the glacier to grow and advance into the fjord. This unrealistic low value for ELA is chosen to provide an extreme positive mass balance to produce the glacier's greatest extent. Figure 4 presents the evolution of glacier length over time simulated by the water depth model (solid curve) and the flotation model (dashed curve). For both model formulations the glacier grows and reaches a maxi-

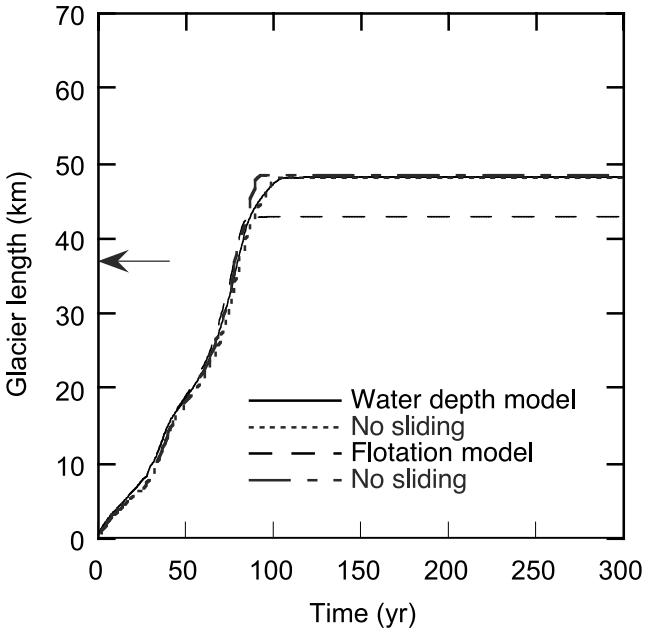

Figure 4. Evolution of the glacier length with time. Formation of moraine shoal is not considered in the model. The arrow at 37 km indicates where the bed falls below sea level.

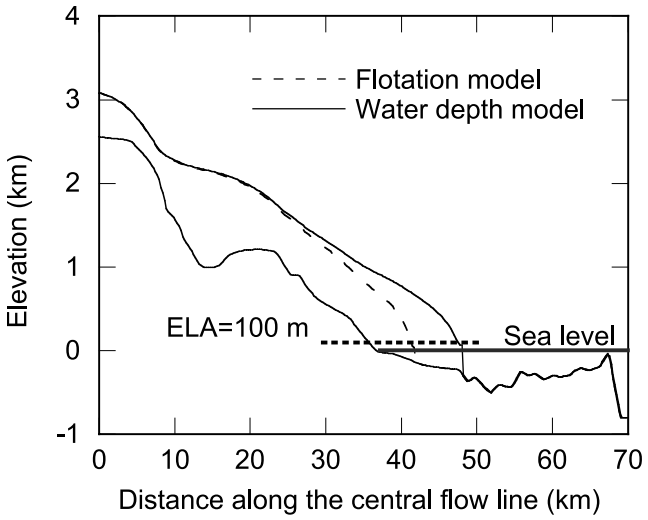

Figure 5. Glacier surface profile at maximum extent, simulated by the flotation model (dashed curve) and the water depth model (solid curve). Sedimentation is not included.

mum extent. Corresponding surface profiles at maximum extent are depicted in Figure 5. As the glacier terminus advances into deep water, the calving flux increases and balances forward movement of the terminus associated with ice flow, prohibiting further glacier advance. The maximum glacier extent is greater in the water depth model than the flotation model. In the flotation model, when the terminus encounters deeper water, the frontal thickness is not large enough to satisfy the flotation criterion, and therefore the terminus retreats and does not advance as far as in the water depth model.

[27] The short-dashed and long-short-dashed curves in Figure 4 represent the modeled glacier length without sliding for the water depth and the flotation models, respectively. Omitting basal sliding allows the glacier to become thicker in the terminal region. A thicker terminus and larger surface slope increase the deformation velocities in that region, and consequently, the glacier advances at more or less the same rate as when sliding is included. For the flotation model, changes are more significant as the calving is related to glacier thickness. In this model, when there is no sliding, the glacier terminus gets thicker; thus calving decreases, and the glacier advances into deeper water.

[28] Neither of the model formulations allows the glacier to advance into water with a depth greater than ~300 m and to reach the end of the fjord. This suggests that irrespective of the calving criterion and surface mass balance, to allow the terminus of a tidewater glacier to advance the full length of the fjord, either the fjord must be comparatively shallow (less than ~300 m water depth) or sedimentary processes must play a role.

4.2. Glacier Advance With Moraine Bank

[29] The next experiments incorporate sediment transport and deposition into the ice flow model. Glacier advance is initiated by applying a more realistic ELA = 900 m (mean value during the Little Ice Age). An average erosion rate (q = 4 mm yr^{-1}) is used in the sediment model. The evolution of the glacier surface during the advance phase for the water depth and flotation models is shown in Figure 6a and 6b, respectively. The time interval between profiles is 20 years. Advance into deeper water becomes possible because the sediment shoal (gray outgrowths on the bed topography, Figure 6) reduces water depth and restricts calving. The glacier starts advancing when sedimentation at the terminus reduces the local water depth to around 250–300 m. Figure 7 illustrates the glacier length variation over time. While the glacier is advancing, the calving front reaches deeper water, leading to higher calving flux and slower advance. Where a basal depression (at 49 km and 51 km, Figure 6) is present, the glacier advances very slowly or remains steady until the depression is filled with sediment and water depth decreases sufficiently to allow the terminus to advance again. For the chosen α = 10 yr^{-1} and q_0 = 0.15, glacier advance according to the flotation model (long-

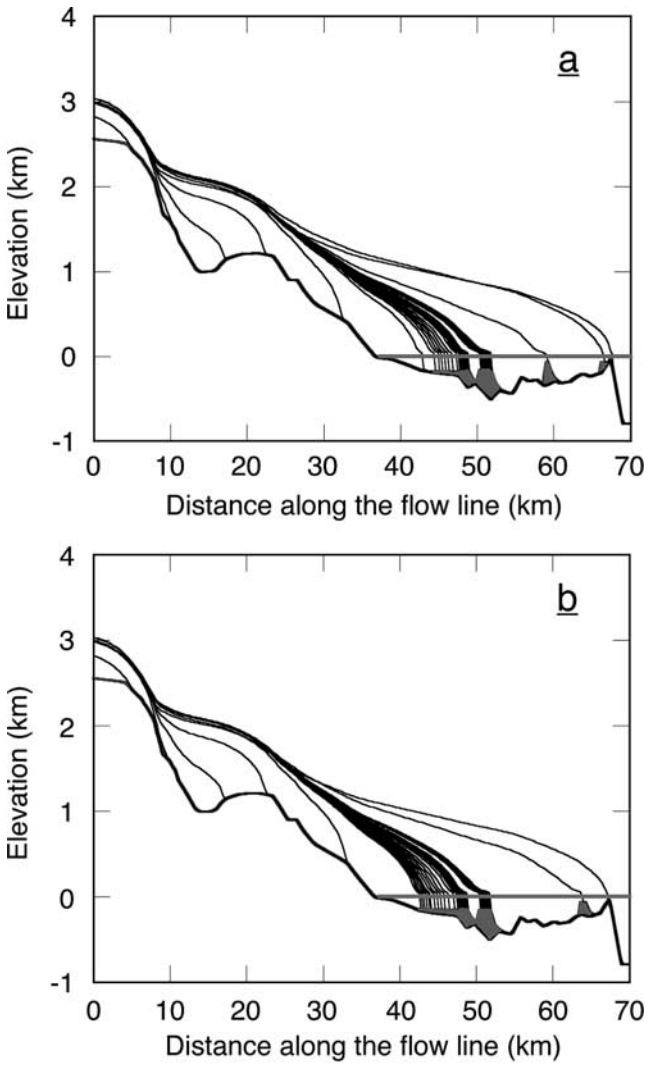

Figure 6. Evolution of the glacier surface, including sedimentation, during the advance for (a) the water depth model and (b) the flotation model. The moraine shoal grows and moves forward as the glacier advances. The time interval between profiles is 20 years.

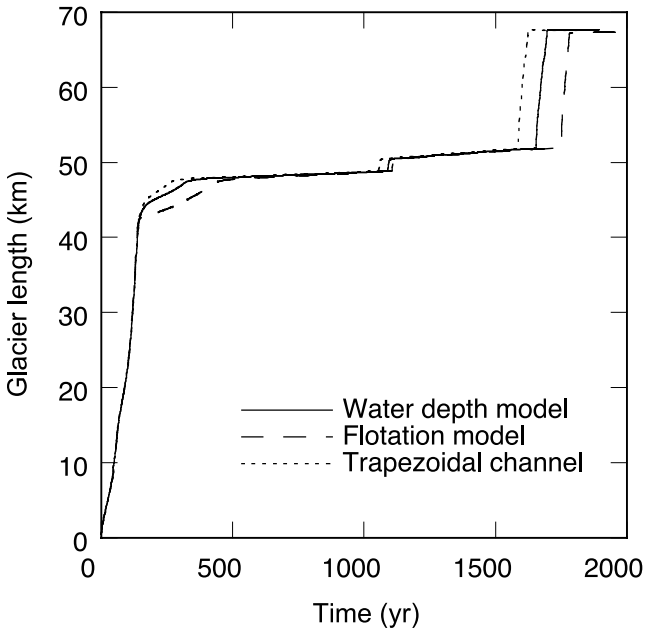

Figure 7. Simulated evolution of glacier length over time, assuming a moraine shoal in front of the glacier.

dashed curve) is slightly slower than for the water depth model (solid curve) because a somewhat higher moraine bank (smaller water depth) is required to satisfy the flotation criterion (Figure 7). The short-dashed curve in Figure 7 represents glacier length assuming a trapezoidal geometry for the channel cross section. Using this geometry implies a narrower channel for the thinner glacier tongue. As the glacier thickens, the glacier width increases. The onsets of rapid advances occur earlier for the trapezoidal channel geometry (short-dashed curve) than for the rectangular channel geometry (solid curve), but otherwise predicted glacier evolution is very similar (Figure 7). Therefore the rectangular channel geometry is used in all subsequent model experiments.

4.3. Sensitivity of Model Results

[30] Additional model runs with different average erosion rates are performed to examine the sensitivity of the modeled glacier to the amount of sedimentation (Figure 8). In all runs, ELA = 900 m is specified. Varying the sediment rate has a substantial effect on advance rate, as would be expected: Higher sedimentation (q = 8 mm yr^{-1}) reduces water depth in a shorter time, so calving rate decreases faster and the glacier can advance more rapidly (short-dashed curve), whereas a lower sedimentation rate (q = 2 mm yr^{-1}) leads to a slower advance (long-dashed curve). In both cases, however, the terminus reaches the end of the fjord (Figure 8).

[31] To examine the sensitivity of the modeled glacier to climate forcing, the model is run with a warmer climate (ELA = 1100 m, corresponding to the present climate) and a cooler climate (ELA = 700 m). The same average erosion rate (q = 4 mm yr^{-1}) is used. Modeled advance for different runs is illustrated in Figure 9 and shows that advance rates during the rapid and slow phases are not affected significantly by the ELA but the onset of these phases is shifted in time. As the terminus advances into deeper water (>250 m), the glacier becomes relatively insensitive to climate change. From this we conclude that climate forcing had smaller effect on the advance of Columbia Glacier than the formation of the moraine bank.

5. Discussion

[32] Figure 10 illustrates the terminus position reconstructed from tree ring data along the west and east margins of Columbia Fjord [*Kennedy*, 2003]. Glacier advance started

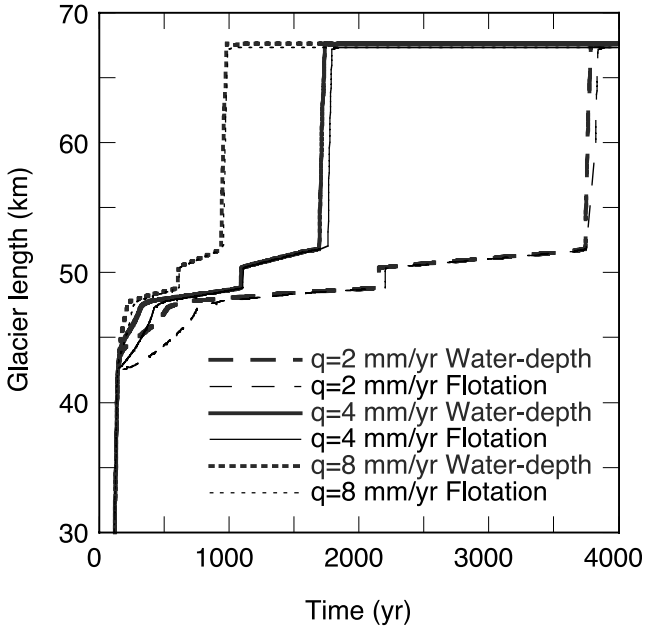

Figure 8. Glacier length sensitivity to the average erosion rate.

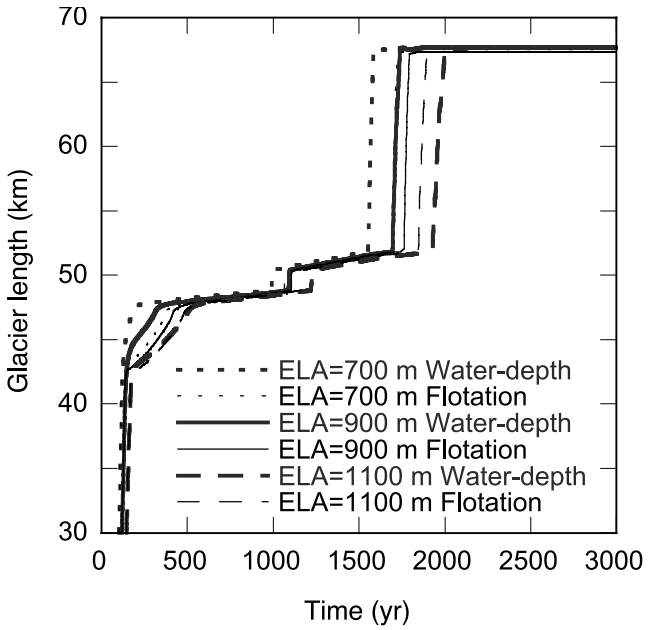

Figure 9. Glacier length sensitivity to ELA.

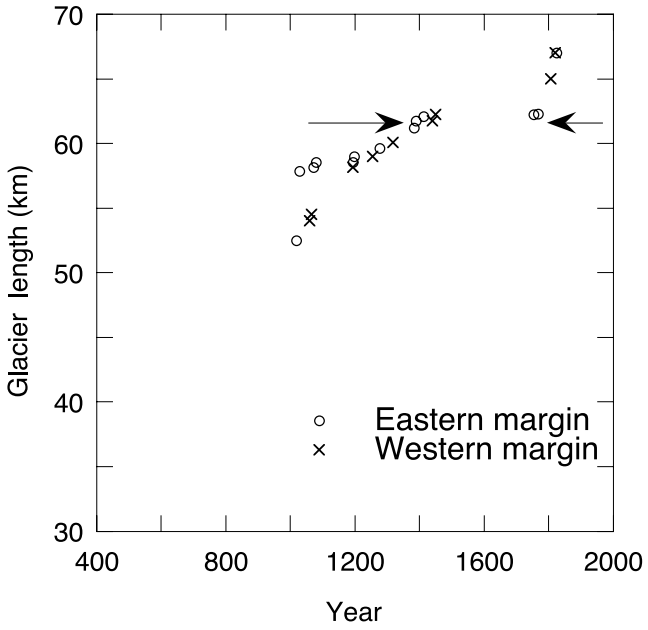

Figure 10. Position of the glacier front along its margins in Columbia Bay, obtained from tree ring data. The arrows show the location where the terminus remained steady for nearly three centuries.

in the mid-A.D. 1000s, experienced a stillstand or possibly retreat at 61 km from ~A.D. 1450 to 1750 (arrows in Figure 10), followed by another advance to the maximum extent reached at ~A.D. 1800. At 61 km the glacier advances over a bed that shallows along the flow line; therefore decreased calving would be expected, facilitating terminus advance rather than the inferred stand still. Without invoking some external mechanism a steady terminus position at this location or even terminus retreat is rather unlikely [*Nick and Oerlemans*, 2006]. The cause of the inferred phase of steady terminus position is unknown but could be related to climate forcing or to a change in proglacial sedimentation.

[33] The first modeling attempts to produce the observed terminus behavior involved climate forcing. Maintaining a stationary terminus at 61 km for a period of 300 years requires a substantial increase in ELA around A.D. 1400 followed by a lowering of the ELA after about two centuries. This would indicate that the glacier experienced a very warm climate starting around A.D. 1400. However, the available climate record for this region spanning the last millennium indicates a cool period around A.D. 1400 [*Barclay et al.*, 1999; *Wiles et al.*, 2004]. Figure 11a represents the tree ring chronology of Columbia Bay; a large mean ring width indicates high growth rate and is interpreted as favorable climate conditions. Therefore a decrease in ring width is consistent with cooling conditions. The record shown in Figure 11a suggests colder climate conditions during the 15th century, which is opposite to the warming required to maintain the terminus at 61 km. To further investigate the effect of climate forcing on glacier advance, the water depth model is run by applying a climate forcing proportional to the tree ring width. The experiment is done for different constant of proportionality between ELA and the tree ring width. The simulated glacier length does not show any steady state around 61 km and is also insensitive to the constant of proportionality (Figure 11b). Consequently, observed behavior of the glacier terminus between A.D. 1400 and 1700 is unlikely to reflect changing climate conditions.

[34] The observed steady terminus position might have occurred because of a substantial change in height of the moraine bank when the glacier reached this location. Inspection of the geometry of the fjord (Figure 12) suggests that part of the sediment may initially have been diverted into the open areas along both margins. Arrows in Figure 12 illustrate possible directions for the sediment transport. This lateral transport would have resulted in a reduction of the shoal height and, consequently, an increase in calving rate, temporarily halting glacier advance. The terminus remained

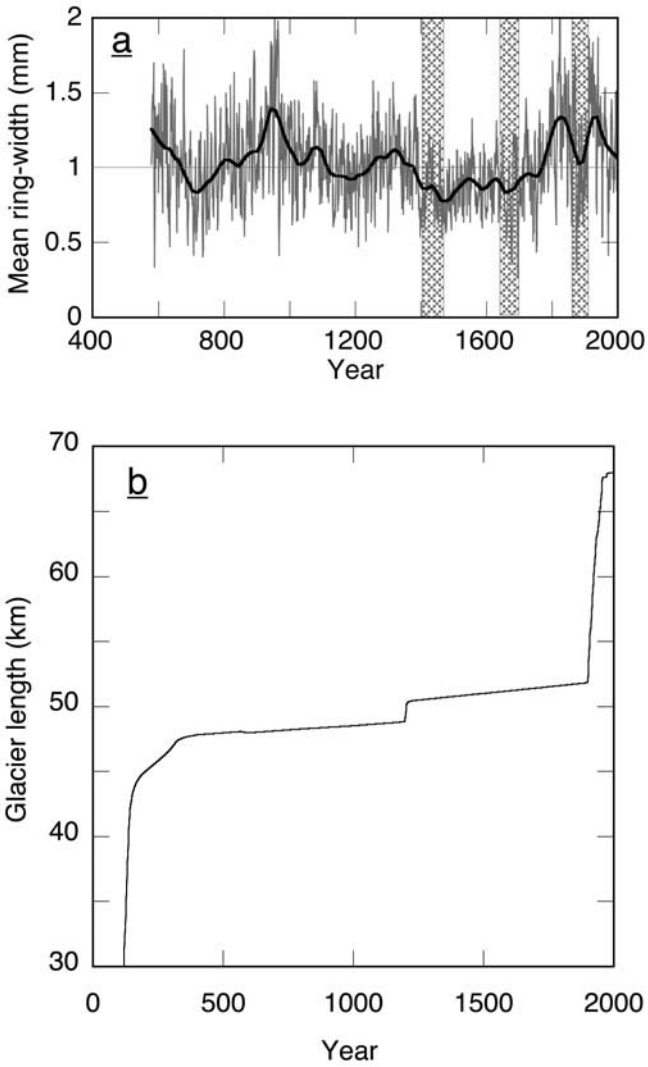

Figure 11. (a) Columbia Bay tree ring chronology through the last 1400 years. The bold curve is made by the weighted curve-fitting method. The shaded bars indicate the cool intervals around A.D. 1400, 1600, and 1870 (G. C. Wiles, personal communication, 2005). (b) Glacier length simulated with the water depth model. Mass balance forcing is proportional to tree ring width variation.

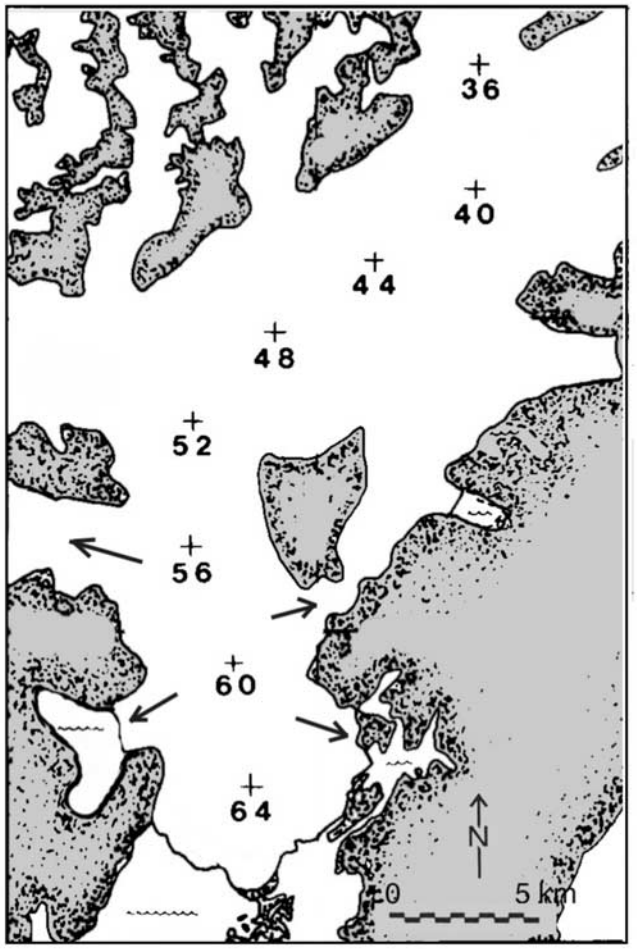

Figure 12. Map of Columbia Fjord. Numbers indicate the distance from the head of the glacier along the central flow line. Arrows show approximate directions of the sediment movement.

at this location until the height of the sediment shoal increased sufficiently to reduce calving rate.

[35] Figure 13 shows modeled glacier length predicted by the water depth model with ELA = 900 m and $q = 4$ mm yr^{-1}. Assuming that the total amount of sediment, Q in equation (11), decreases about 50% at 60 km due to lateral diversion, the glacier stops advancing around A.D. 1400 (arrows in Figure 13), and the terminus position remains steady or retreats slightly until the shoal becomes high enough to reduce calving and to allow further glacier advance. The results qualitatively agree with the observed terminus positions shown in Figure 10.

[36] Another possible explanation is that the glacier bed topography was different during glacier advance. Existence of any basal depression around 61 km would provide a steady state phase until the glacier builds a large enough moraine bank to decrease water depth and to advance further. It is possible that a part of the moraine bank, which filled the basal depression, was not excavated during subsequent glacier advance, resulting in the observed upward slope instead of basal over deepening.

[37] *Van der Veen and Whillans* [1993] showed that less than 20% of the flow resistance of Columbia Glacier is due to the lateral drag and gradients in longitudinal stress. Therefore we did not include longitudinal stress gradients and lateral drag in our model. It should also be noted that we did not account for potential restraining forces associated with the sediment bank [*Fischer and Powell*, 1998]. The sedimentation model used in this study is a simple first approximation. For further refinement it is necessary to use a more realistic model and also to obtain data, which reveal the possible shape and size of the moraine shoal and how this shoal affects the forward motion of the glacier.

[38] The detailed history of the terminus of Columbia Glacier at the end of the fjord is rather complex with small advances and retreats occurring in the late 1800s and early 1900s [*Gilbert*, 1904; *Grant and Higgins*, 1913]. The reason that advance of Columbia Glacier was halted at Heather Island might be linked to climate fluctuations or to the geometry of the bay behind the island. In this study we did not investigate under what conditions the glacier stopped advancing and, instead, assumed a rapid increase in water depth beyond the fjord (which effectively prevents the terminus from advancing further). More detailed investigations concerning processes that may have halted advance and initiated retreat requires more complete data including high-resolution climate history, sedimentation rate, and the bathymetry of Columbia Bay.

6. Conclusions

[39] The present model study indicates that the terminus of a tidewater glacier cannot advance into water deeper than ~300 m unless sedimentation at the glacier front is included. This finding confirms earlier suggestions concerning the importance of proglacial sedimentation in allowing tidewater glaciers to advance down the fjord [e.g., *Post*, 1975; *Powell*,

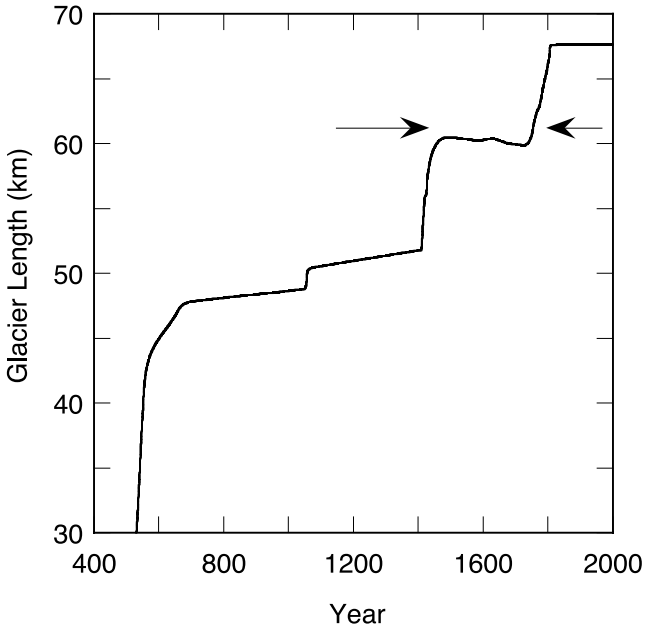

Figure 13. Simulated glacier length with the water depth model. The arrows mark the steady state due to lateral diversion of sediments.

1991]. Irrespective of the accumulation rate and the calving criteria (the water depth model or the flotation model), it is impossible to reproduce glacier advance into deeper water.

[40] We incorporated a simple sediment transport scheme into the numerical ice flow model. As the glacier advances, the sediment bank at the calving front is pushed forward in a conveyor belt fashion with the bank size continually increasing due to the addition of sediments eroded up glacier and transported to the terminus. The model simulations show that the glacier can advance only if sedimentation at the glacier front reduces the local water depth to around 250–300 m.

[41] The observed advance of Columbia Glacier is qualitatively reproduced by prescribing a constant mass balance and varying sediment bank height in front of the terminus. Comparison of model experiments with the climate record for the last millennium indicates that major changes in glacier advance (300 years of near steady terminus position halfway in the fjord) are unlikely related to climate change. The advance of Columbia Glacier is largely the result of the formation and evolution of a terminal moraine rather than changes in climate. These findings suggest that during the prolonged phase of advance down the fjord the response of a tidewater terminus to climate change may be of secondary importance compared to the rate of growth and migration of a terminal moraine. Therefore it is important to understand and consider these processes when interpreting glacier behavior as an indicator of climatic fluctuations.

[42] Two calving models were implemented into the ice flow model as lower boundary condition, one based on the correlation between water depth and calving rate and the other based on the flotation criterion proposed by *van der Veen* [1996] in which the terminus retreats to where the frontal thickness is greater than the flotation thickness by a prescribed amount. Both models yield similar glacier behavior. With the presently available data for the advance of Columbia Glacier it is not possible to decide unambiguously in favor of either of these models.

[43] **Acknowledgments.** The authors are grateful to Gregory Wiles and Shad O'Neal for providing data. We also thank Tad Pfeffer for helpful comments and suggestions. C.J.V. acknowledges support from the National Science Foundation through grant NSF-ARC 0520427.

References

Abdalati, W., W. Krabill, E. Frederick, S. Manizade, C. Martin, J. Sonntag, R. Thomas, W. Wright, and J. Yungel (2001), Outlet glacier and margin elevation changes: Near coastal thinning of the Greenland Ice Sheet, *J. Geophys. Res.*, *106*, 33,729–33,741.

Alley, R. B. (1991), Sedimentary processes may cause fluctuations of tidewater glaciers, *Ann. Glaciol.*, *15*, 119–124.

Alley, R. B. (1992), Flow-law hypotheses for ice-sheet modelling, *J. Glaciol.*, *38*, 245–256.

Barclay, D. J., G. C. Wiles, and P. E. Calkin (1999), A 1119-year tree-ring-width chronology from western Prince William Sound, southern Alaska, *Holocene*, *9*, 79–84.

Bindschadler, R. (1983), The importance of pressurized subglacial water in separation and sliding at the glacier bed, *J. Glaciol.*, *29*, 3–19.

Brown, C. S., M. F. Meier, and A. Post (1982), Calving speed of Alaska tidewater glaciers, with application to Columbia Glacier, *U.S. Geol. Surv. Prof. Pap.*, *1258C*.

Budd, W. F., P. L. Keage, and N. L. Blundy (1979), Empirical studies of ice sliding, *J. Glaciol.*, *23*, 157–170.

Calkin, P. E., G. C. Wiles, and D. J. Barclay (2001), Holocene coastal glaciation of Alaska, *Quat. Sci. Rev.*, *20*, 449–461.

Clarke, G. K. C. (1987), Fast glacier flow: Ice streams, surging, and tidewater glaciers, *J. Geophys. Res.*, *92*, 8835–8841.

Fischer, M. P., and R. D. Powell (1998), A simple model for the influence of push-morainal banks on the calving and stability of glacial tidewater termini, *J. Glaciol.*, *44*, 31–41.

Fountain, A. G. (1982), Columbia Glacier photogrammetric altitude and velocity: Data set (1957–1981), *U.S. Geol. Surv. Open File Rep.*, *82–756*.

Gilbert, G. (1904), *Glaciers and Glaciation*, *Harriman Alaska Ser.*, vol. 3, 231 pp., Doubleday Page, Washington, D. C.

Glen, J. W. (1955), The creep of polycrystalline ice, *Proc. R. Soc. London, Ser. A*, *228*, 519–538.

Grant, U. S., and D. Higgins (1913), Coastal glaciers of Prince William Sound and Kenai Peninsula, *U.S. Geol. Surv. Bull.*, *526*, 1–75.

Hanson, B., and R. L. Hooke (2000), Glacier calving: A numerical model of forces in the calving speed-water depth relation, *J. Glaciol.*, *46*, 188–194.

Hanson, B., and R. L. Hooke (2004), Buckling rate and overhang development at a calving face, *J. Glaciol.*, *49*, 577–586.

Hughes, T. J. (1992), Theoretical calving rates from glaciers along ice walls grounded in water of variable depths, *J. Glaciol.*, *38*, 282–294.

Hughes, T. J., and J. L. Fastook (1997), The relationship between calving rates, ice velocities and water depth, in *Calving Glaciers: Report of a Workshop, February 28–March 2, 1997*, edited by C. J. van der Veen, *BPRC Rep. 15*, pp. 77–84, Byrd Polar Res. Cent., Ohio State Univ., Columbus.

Hunter, L. E., R. D. Powell, and D. E. Lawson (1996a), Morainal-bank sediment budgets and their influence on the stability of tidewater termini of valley glaciers entering Glacier Bay, Alaska, U.S.A., *Ann. Glaciol.*, *22*, 211–216.

Hunter, L. E., R. D. Powell, and D. E. Lawson (1996b), Flux of debris transported by ice at three Alaskan tidewater glaciers, *J. Glaciol.*, *42*, 123–135.

Iken, A. (1981), The effect of the subglacial water pressure on the sliding velocity of a glacier in an idealized numerical model, *J. Glaciol.*, *27*, 407–421.

Joughin, I., W. Abdalati, and M. Fahnestock (2004), Large fluctuations in speed on Greenland's Jokobshaven Isbrae Glacier, *Nature*, *432*, 608–610.

Kamb, B., H. Engelhardt, M. A. Fahnestock, N. Humphrey, M. Meier, and D. Stone (1994), Mechanical and hydrologic basis for the rapid motion of a large tidewater glacier: 2. Interpretation, *J. Geophys. Res.*, *99*, 15,231–15,244.

Kennedy, M. G. (2003), Advance rates of Columbia Glacier during the last 1000 years, Prince William Sound, Alaska, M.S. thesis, 45 pp., Coll. of Wooster, Wooster, Ohio.

Krimmel, R. M. (1987), Columbia Glacier, Alaska: Photogrammetry data set (1981–82 and 1984–85), *U.S. Geol. Surv. Open File Rep.*, *87–219*.

Krimmel, R. M. (1992), Photogrammetric determinations of surface altitude, velocity and calving rate of Columbia Glacier, Alaska, 1983–91, *U.S. Geol. Surv. Open File Rep.*, *92104*.

Krimmel, R. M. (1997), Documentation of the retreat of Columbia Glacier, Alaska, in *Calving Glaciers: Report of a Workshop, February 28–March 2, 1997*, edited by C. J. van der Veen, *BPRC Rep. 15*, pp. 105–108, Byrd Polar Res. Cent., Ohio State Univ., Columbus.

Krimmel, R. M. (2001), Photogrammetric data set, 1957–2000, and bathymetric measurements for Columbia Glacier, Alaska, *U.S. Geol. Surv. Water Resour. Invest. Rep.*, *014089*, 40 pp.

Lingle, C. S., and T. J. Brown (1987), A subglacial aquifer bed model and water pressure dependent basal sliding relationship for a West Antarctic ice stream, in *Dynamics of the West Antarctic Ice Sheet*, edited by C. J. van der Veen and J. Oerlemans, pp. 249–285, Reidel, Dordrecht, Netherlands.

Mayo, L., D. Trabant, R. March, and W. Haeberli (1979), Columbia Glacier stake location, mass balance, glacier surface altitude, and ice radar data—1978 measurement year, *U.S. Geol. Surv. Open File Rep.*, *79-1168*, 79 pp.

Meier, M. F. (1994), Columbia Glacier during rapid retreat: Interactions between glacier flow and iceberg calving dynamics, in *Workshop on the Calving Rate of West Greenland Glaciers in Response to Climate Change*, edited by N. Reeh, pp. 63–83, Dan. Polar Cent., Copenhagen.

Meier, M. F. (1997), The iceberg discharge process: Observations and references drawn from the study of Columbia Glacier, in *Calving Glaciers: Report of a Workshop, February 28–March 2, 1997*, edited by C. J. van der Veen, *BPRC Rep. 15*, pp. 109–114, Byrd Polar Res. Cent., Ohio State Univ., Columbus.

Meier, M. F., and A. Post (1987), Fast tidewater glaciers, *J. Geophys. Res.*, *92*, 9051–9058.

Meier, M. F., L. A. Rasmussen, R. M. Krimmel, R. W. Olsen, and D. Frank (1985), Photogrammetric determination of surface altitude, terminus position, and ice velocity of Columbia Glacier, *U.S. Geol. Surv. Prof. Pap.*, *1258-F*, 41 pp.

Meier, M. F., et al. (1994), Mechanical and hydrologic basis for the rapid motion of a large tidewater glacier: 1. Observation, *J. Geophys. Res.*, *99*, 15,219–15,229.

Mercer, J. H. (1961), The response of fjord glaciers to changes in the firn limit, *J. Glaciol.*, *3*, 850–858.
Nick, F. M., and J. Oerlemans (2006), Dynamics of tidewater glaciers: Comparison of three models, *J. Glaciol.*, *52*, 183–190.
Nye, J. F. (1965), The flow of a glacier in a channel of rectangular, elliptic, or parabolic cross-section, *J. Glaciol.*, *5*, 661–690.
Oerlemans, J. (2001), *Glaciers and Climate Change*, 148 pp., A. A. Balkema, Amsterdam.
Oerlemans, J., and F. Nick (2006), Modelling the advance-retreat cycle of a tidewater glacier with sediment dynamics, *Global Planet. Change*, *50*, 148–160.
O'Neel, S., W. T. Pfeffer, R. Krimmel, and M. Meier (2006), Evolving force balance at Columbia Glacier, Alaska, during its rapid retreat, *J. Geophys. Res.*, *110*, F03012, doi:10.1029/2005JF000292.
Paterson, W. S. B. (1981), *The Physics of Glaciers*, Pergamon, Oxford, U. K.
Pelto, M. S., and C. R. Warren (1991), Relationship between tidewater glacier calving velocity and water depth at the calving front, *Ann. Glaciol.*, *15*, 115–118.
Pfeffer, W., J. Cohn, M. Meier, and R. Krimmel (2000), Alaskan glacier beats a rapid retreat, *Eos Trans. AGU*, *81*, 577.
Post, A. (1975), Preliminary hydrology and historic terminal changes of Columbia Glacier, Alaska, *U.S. Geol. Surv. Hydrol. Invest. Atlas*, *559*, 3 pp.
Powell, R. D. (1990), Glacimarine processes at grounding-line fans and their growth to ice-contact deltas, in *Glacimarine Environments: Processes and Sediments*, edited by J. A. Dowdeswell and J. D. Scourse, pp. 53–57, Geol. Soc., London.
Powell, R. D. (1991), Grounding-line systems as second-order controls on fluctuations of tidewater termini of temperate glaciers, *Spec. Pap. Geol. Soc. Am.*, *261*, 75–93.
Reeh, N. (1968), On the calving of ice from floating glaciers and ice shelves, *J. Glaciol.*, *7*, 215–232.
Sikonia, W. G. (1982), Finite-element glacier dynamics model applied to Columbia Glacier, Alaska, *U.S. Geol. Surv. Prof. Pap.*, *1258B*, 74 pp.
Tangborn, W. (1997), Using low-altitude meteorological observations to calculate the mass balance of Alaska's Columbia and relate it to calving and speed, in *Calving Glaciers: Report of a Workshop, February 28–March 2, 1997*, edited by C. J. van der Veen, *BPRC Rep. 15*, pp. 14–161, Byrd Polar Res. Cent., Ohio State Univ., Columbus.
van der Veen, C. J. (1995), Controls on calving rate and basal sliding: Observations from Columbia Glacier, Alaska, prior to and during its rapid retreat, 1976–1993, *BPRC Rep. 11*, 72 pp., Byrd Polar Res. Cent., Ohio State Univ., Columbus.
van der Veen, C. J. (1996), Tidewater calving, *J. Glaciol.*, *42*, 375–385.
van der Veen, C. J. (1999), *Fundamentals of Glacier Dynamics*, 460 pp., A. A. Balkema, Rotterdam, Netherlands.
van der Veen, C. J., and A. J. Payne (2004), Modelling land-ice dynamics, in *Mass Balance of the Cryosphere*, edited by J. L. Bamber and A. J. Payne, pp. 169–226, Cambridge Univ., Cambridge, U. K.
van der Veen, C. J., and I. Whillans (1993), Location of mechanical controls on Columbia Glacier, Alaska, U.S.A., prior to its rapid rereat, *Arct. Alp. Res.*, *25*, 99–105.
Vieli, A., M. Funk, and H. Blatter (2001), Flow dynamics of tidewater glaciers: a numerical modelling approach, *J. Glaciol.*, *47*, 595–606.
Viens, R. J. (1995), Dynamics and mass balance of tidewater calving glaciers of southern Alaska, M. S. thesis, Univ. of Wash., Seattle.
Weertman, J. (1964), The theory of glacier sliding, *J. Glaciol.*, *5*, 287–303.
Wiles, G. C., R. D. D'Arrigo, R. Villalba, P. E. Calkin, and D. J. Barclay (2004), Century-scale solar variability and Alaskan temperature change over the past millennium, *Geophys. Res. Lett.*, *31*, L15203, doi:10.1029/2004GL020050.

F. M. Nick, Department of Geography, University of Durham, South Road, Durham DH1 3LE, UK. (faezeh.nick@durham.ac.uk)
J. Oerlemans, Institute for Marine and Atmospheric Research Utrecht, Princetonplein 5, NL-3584 CC Utrecht, Netherlands.
C. J. van der Veen, Department of Geography, University of Kansas, Lawrence, KS 66045, USA.